Int. J. Electrochem. Sci., 12 **(2017)** 10605 – 10615, doi: 10.20964/2017.11.62

International Journal of ELECTROCHEMICAL SCIENCE
www.electrochemsci.org

Fabrication of a Chitosan-Iron Oxide Nanocomposite for Electrochemical Detection of Trace Cadmium in Orchard Soil in the Loess Plateau

Qi Zhang[1,2], Yan'an Tong[1,2], Lili Yang[1,2], Gaoyuan Liu[1,2], Lianyou Liang[1,2], Wenshe Han[1,2] and Ming Zhang[3]*

[1] College of Natural Resources and Environment, Northwest A & F University, Yangling, Shaanxi, 712100, China
[2] Key Laboratory of Plant Nutrition and the Agri-environment in Northwest China, Ministry of Agriculture, Shaanxi 712100, China
[3] College of Chemistry and Material Science, Sichuan University, 610064, China
[*]E-mail: shaanxizhangqi@163.com

Received: 25 July 2017 / *Accepted:* 10 September 2017 / *Published:* 12 October 2017

In this work, a chitosan-iron oxide nanocomposite (CHIT-IO) film was deposited onto fluorine tin oxide (FTO) to yield an electrochemical sensor to detect trace level cadmium. UV–visible spectroscopy and Fourier transform infrared spectroscopy (FTIR) were used to measure the iron oxide nanoparticles (IONPs) prepared via a co-precipitation technique. The increased electron transportation rate and remarkable electrochemical behaviour were confirmed for the synthesized electrode. Under optimum conditions, the stripping peak currents were linearly related to the concentration of the Cd(II) (1.0—100.0 μg/L), and a limit of detection (LOD) of 0.15 μg/L was obtained. The proposed electrode was then used for Cd(II) detection in soil extracts, and the desirable results are provided herein. The results indicate the proposed electrochemical determination method shows a comparable performance compared with that of the ICP-MS method.

Keywords: Electrochemical sensor; Chitosan; Iron oxide; Fluorine tin oxide; Cadmium; Soil

1. INTRODUCTION

Cadmium is widely acknowledged to be a hazard to the environment and to cause extreme toxicity to diverse organs and systems in humans and animals [1, 2]. Cd pollution occurred widely in China resulting from its rapidly economic development during the past two decades [3, 4]. Therefore, the potential health risks of Cd contamination in some fruits orchard, such as pear, grape, apple, and

orange, have been assessed in China [5, 6]. To protect human health, the maximal contaminant level in standard drinking water of 10 μg/L was recommended by the US Environmental Protection Agency. Techniques for Cd(II) detection have been widely explored considering its extreme harm to human health and increased industrial applications. According to the Chinese (HJ/T 332-2006 Environmental quality evaluation standards for farmland of edible agricultural products， the Cd limitation should be lower or equal 0.6mg/kg in the orchard soil in the loess plateau soil with the pH≥7.5. Hence, green, effective, selective and facile techniques are expected to be developed for Cd(II) detection in both biological and environmental specimens [7-11]. In spite of the accuracy in cadmium detection, techniques like ICP-OES, ICPMS and AAS are poorly efficient and time-consuming and require expensive instrumentation and maintenance. In addition, fast monitoring of heavy metals to characterize contaminated sites could not be suitably addressed by these techniques. Electro-analyses, especially a stripping analysis, are regarded as the popular candidates for cadmium detection. Anodic stripping voltammetry (ASV) is remarkably selective and sensitive and is considered the most appealing electrochemical method for the determination of heavy metals at trace levels. Furthermore, the instrumentation required for ASV measurements is simple, portable, suitable for automation, low in electrical power consumption and comparatively cheap [12-14].

Generally, the electrode material is a key factor that prominently affects the behaviour in ASV. An ideal electrode should be electrochemically and chemically inert and have a low background current and ohmic resistance, high oxygen and hydrogen overpotentials with a broad potential window, and desirable mechanical features. Additionally, its surface should be easily reproducible. Electrochemical biosensors have enhanced biological and chemical sensing due to the use of nanoparticles [15-23], and iron oxide [24, 25], zinc oxide [26], cerium oxide [27-29] and other metal oxide nanoparticles have been proposed as remarkable matrices for sensing applications of desired biomolecules. Since IONPs with ultra-paramagnetism are characteristic of signal amplification and a desirable microenvironment for protein adhesion and can promote conductivity, they promote selectivity and sensitivity as an electrochemical transducer. Furthermore, IONPs are desirable for biosensor applications after they are dispersed in a biopolymer matrix of CHIT, which addresses the aggregation and fast biodegradation of IONPs in a given matrix containing biomolecules. CHIT excels in comparison with other polymers and has attracted increasing attention because it is biodegradable and biocompatible. In addition, the material with a specific functionality would be flexible since —NH_2 and —OH groups exist on CHIT [30-34].

In recent years, FTO glass sheets have attracted attention as a solid support during the fabrication of electrochemical biosensors [35, 36]. FTO sheets are remarkably resistant at high temperatures, visibly transparent, mechanically strengthened, chemically inert, relatively stable in atmospheric circumstances, cost effective and electrically conductive. Moreover, diffusion is eliminated by the sheets, as shown in the case of the ITO sheets.

In this study, a CHIT-IO film was deposited onto FTO to yield an electrochemical sensor to detect cadmium in real specimens. The results obtained from a series of experiments indicated that the proposed electrode is remarkably sensitive, repeatable, mechanically stable, and resistant to surfactant interferences with a low background current.

2. EXPERIMENTS

2.1. Reagent

Ferric chloride hexahydrate, ferrous chloride tetrahydrate, chitosan and fluorine-doped tin oxide (FTO) sheets were commercially available from Sigma-Aldrich. The 1,000 mg/L Cd(II) stock solution was supplied by the National Standard Reference Materials Centre of China and was later diluted as needed.

2.2. Preparation of the iron oxide nanoparticle (IONP)-CHIT composite

A chemical co-precipitation technique was employed to prepare the IONPs. Solutions of 2 g of $FeCl_2 \cdot 2H_2O$ in 10 mL of 2 M HCl and 4 g of $FeCl_3 \cdot 6H_2O$ in 10 mL of 2 M HCl were prepared and magnetically stirred at 60 °C for 0.5 h. After being successively added dropwise to 200 mL of an aqueous ammonia solution (1 M) under vigorous stirring for 120 min at 80 °C, the terminal product was obtained as a black precipitate, which suggested the IONPs formed. The pH was tuned to 7.0 after repeated risings of the precipitate with distilled water and methanol. Subsequently, the nanoparticles were dried at the ambient temperature in a vacuum oven for 1 d before they were stored. Then, 50 mg of the IONPs was dissolved in 10 mL of distilled water, and a suspension was obtained and sonicated at ambient temperature for 60 min. Chitosan (3 g) was dissolved in an acetic acid solution (1%). The obtained mixture was then exposed to ultra-sonication for 60 min to obtain a transparent CHIT solution. The IONP suspension and the CHIT solution were mixed together and stirred for 5 h. Then, FTO sheets were dip coated in the as-prepared CHIT-IO hybrid nanocomposite suspension to yield the electrodes (denoted CHIT-IO/FTO). The electrode fabricated without IONPs was denoted CHIT/FTO.

2.3. Characterizations

UV-visible spectroscopy [Shimadzu UV-1800] was employed to characterize the IONPs via the UV-vis spectrum in the wavelength range from 280 to 500 nm. FTIR (Nicolet iS5, Thermo Scientific) was used for the analysis of the surface functional groups on the specimens.

2.4. Electrochemical measurement

This work used a CHI660D electrochemical workstation (Shanghai CH Instruments, China) to perform electrochemical impedance spectroscopy (EIS), square wave anodic stripping voltammetry (SWASV) and cyclic voltammetry (CV). A traditional triple-electrode configuration was employed to construct the electrochemical cell. Herein the working electrode, reference electrode and auxiliary electrode were the modified FTO, Ag/AgCl (3 M KCl) and a platinum wire, respectively. For the EIS measurements, a multi-impedance test configuration was used for the electrochemical impedance spectroscopy analysis. The AC amplitude was 10 mV, and the frequency ranged from 10 kHz to 10 mHz. CV was performed at a scan rate range of 10-300 mV/s, and the potential range was -1.8-0.8 V.

SWASV measurements were also performed with a step potential and pulse amplitude of 2 mV and 50 mV, respectively, and a 50 ms pulse, scan rate of 10 mV/s, sampling time of 20 ms, and 100 ms pulse interval.

2.5. Soil sample preparation

Soil samples were traditionally collected from the 7a nectarine orchard which had been fertilized with chicken waste as amendment compost, in the Fuping Comprehensive Experiment & Demonstration Station（34°42′N， 108°57′E）of Northwest A & F University, Fuping country, Shaanxi province, China. The soil type belongs to cinnamon soil. All the soil samples were well prepared for testing. 0.25 g soil sample was added into a 25 mL polytetrafluoroethylene solution tube. 9 mL HNO_3 and 3 mL $HClO_4$, after shacking, the dispersion was heated at 130 ^oC. After boiling for 1 h, 5 mL HF was added until the solution become yellow colour or transparent. The solid was transferred to 10 mL plastic tube and added to 20 mL. ICP-AES has been used as a comparison method in this study.

3. RESULTS AND DISCUSSION

The IONPs were characterized via the UV–VIS spectrum in Fig. 1. An absorption peak was observed at 359 nm and attributed to the surface plasmon resonance, which suggested the IONPs successfully formed. According to Mallick et al. [37], the absorption bands in region I (250-400 nm) are due to the ligand-to-metal charge-transfer (LMCT) transitions (direct transitions) combined with the contributions from the Fe^{3+} ligand field transitions.

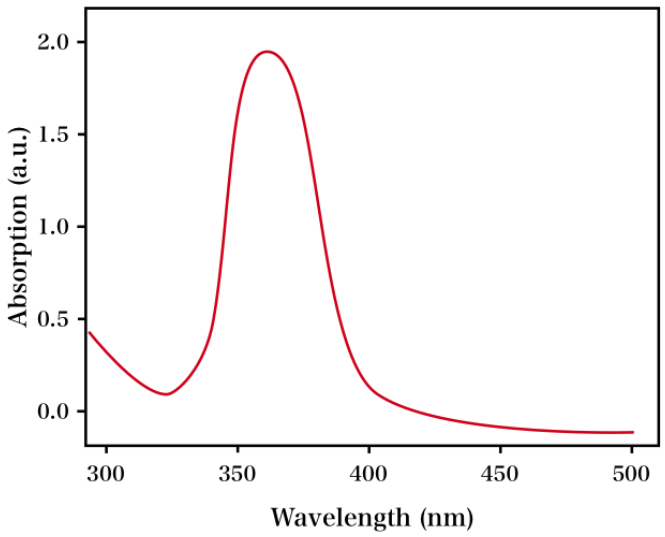

Figure 1. UV–VIS spectrum of the IONPs.

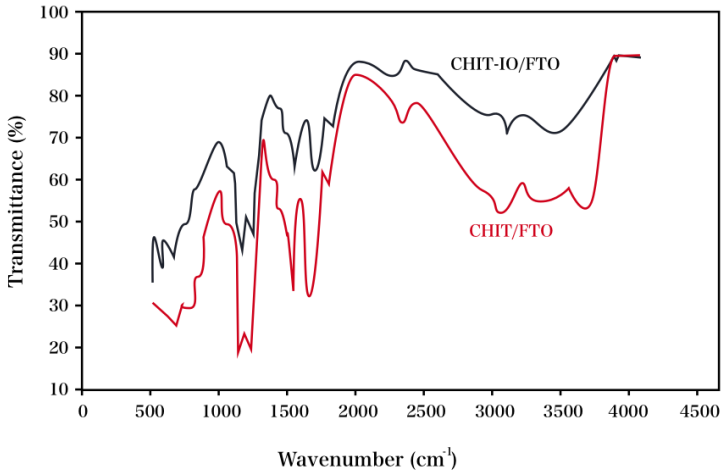

Figure 2. FTIR spectra of CHIT/FTO and CHIT-IO/FTO.

The CHIT/FTO and CHIT-IO/FTO were characterized by the FTIR spectra in Fig. 2. As indicated in the spectrum of the original CHIT, the major peaks were attributed to the stretching vibrations of the –OH groups (2500 to 3500 cm^{-1}) and the overlapping stretching vibrations of the C–H and N–H bonds in the $–CH_3$ groups, which are represented by the peak at 2874 cm^{-1}. The bands observed at 1535 and 1658 cm^{-1} can be explained by the N–H deformation-induced $–NH_2$ group and the amide I band, respectively. The band adjacent to 1156 cm^{-1} is due to the chitosan deacetylation-induced asymmetric vibrations of the –CO in the oxygen bridge. The IR bands that represent the –OH and –NH stretching modes in the FTIR spectrum of CHIT-IO/FTO decreased to lower wavenumbers compared with those of the original CHIT, which suggested the CHIT amine group interacts with the IONPs. The amine groups of the chitosan appeared to bind with the IONPs via electrostatic interactions. The IR band shifted to a lower wavenumber due to the formation of a complex between the surface-charged IONPs and the cationic chitosan matrix, which indicated the formation of the CHIT-IO hybrid nanocomposite [38].

The comparison of the CV responses of the FTO, CHIT/FTO and CHIT-IO/FTO electrodes in an $[Fe(CN)_6]^{3-/4-}$ solution is shown in Fig. 3A. The FTO exhibited a couple of undesirable redox peaks with a peak potential separation of 210 mV, which indicated slow electron transportation at the interface. The undesirable conductivity accounted for this phenomenon. In comparison, the CHIT-IO/FTO exhibited improved and well-defined redox peaks, and the peak potential separation was as small as 89 mV, which suggested significantly enhanced electron transportation at the interface. Compared to the CHIT-IO/FTO, the redox peaks observed in the CV response of the CHIT/FTO under the same conditions were slightly larger, which was possibly because the CHIT film was undesirably conductive. EIS is an effective tool for studying the interface properties of surface-modified electrodes. A typical impedance spectrum (presented in the form of the Nyquist plot) includes a semicircle portion at higher frequencies, corresponding to an electron transfer-limited process, and a linear part in the lower frequency range, representing a diffusion-limited process. Fig. 3B displays the results obtained via the EIS measurements of the interface features of the proposed electrodes. The electron transfer resistances (R_{ct}) values with respect to FTO, CHIT/FTO and CHIT-IO/FTO that were obtained after

fitting the proper circuit were 1320, 544 and 162 Ω, respectively. These results were in good agreement with those recorded from the CV measurements.

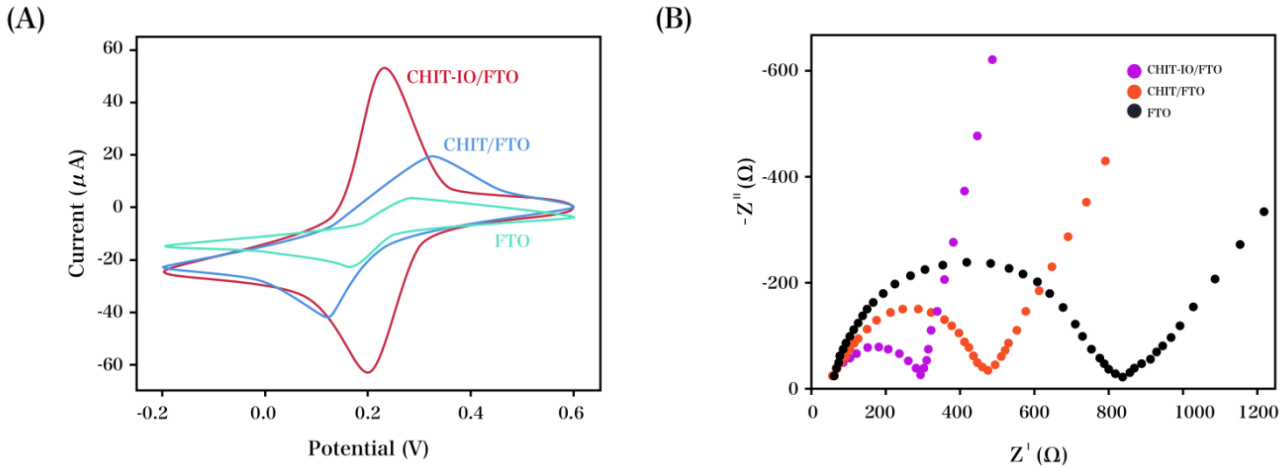

Figure 3. (A) CVs of CHIT-IO/FTO, CHIT/FTO and FTO in $[Fe(CN)_6]^{3-/4-}$ (5 mM) and KCl (0.1 M). (B) Nyquist plots of CHIT-IO/FTO, CHIT/FTO and FTO in $[Fe(CN)_6]^{3-/4-}$ (10 mM) and KCl (0.1 M)

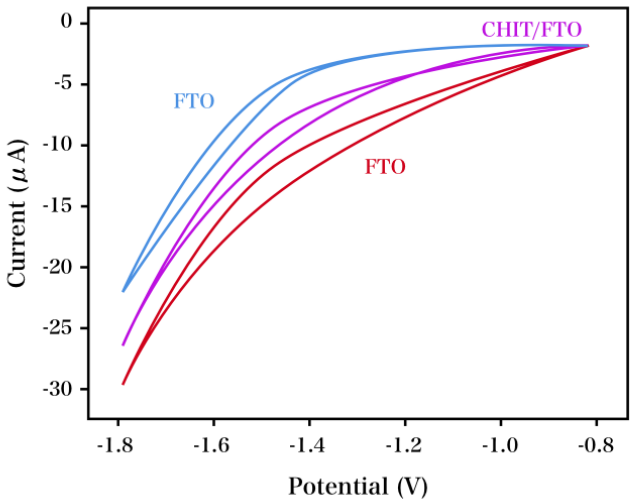

Figure 4. CV scans of CHIT-IO/FTO, CHIT/FTO and FTO in a 0.11 M acetate buffer solution at a pH of 4.0.

The behaviour of the proposed electrode can be greatly affected by the hydrogen evolution process and the background current. The CHIT-IO/FTO, CHIT/FTO and FTO were characterized in an original acetate buffer solution via CV, as shown in Fig. 4, and the FTO electrode exhibited a low background current in the range of −0.7 to −1.1 V. The background current was stable during repetitive scans, which suggested the higher mechanical strength of the CHIT-IO/FTO. Since a CHIT film formed, a comparatively more negative hydrogen evolution potential was observed for the CHIT/FTO electrode than that of the FTO, and a comparatively more negative hydrogen overvoltage was observed

for the CHIT-IO/FTO compared to that of the CHIT/FTO. The synergistic effect of the IONPs and CHIT could account for this variation. As indicated by these results, the CHIT-IO/FTO electrode exhibited an ample reduction potential and a small background current and could be used for a stripping assay.

A comparison of the square wave stripping responses for Cd(II) (20 μg/L) with the FTO, CHIT/FTO and CHIT-IO/FTO electrodes is displayed in Fig. 5A. The original FTO exhibited an insignificant and weak stripping peak for Cd(II) due to its low electrocatalytic activity. In comparison, CHIT/FTO exhibited a higher sensitivity for the determination of Cd(II) than that of FTO, which was possibly due to the promoted non-faradaic preconcentration of metal cations caused by the formation of a cation-exchanger, i.e., a polymeric membrane that formed as a result of the negative charge of the sulfonate groups in the CHIT [39]. Moreover, the CHIT-IO/FTO electrode exhibited the highest peak current, which suggested the incorporation of IO with CHIT further enhanced the electrocatalytic activity of the electrode.

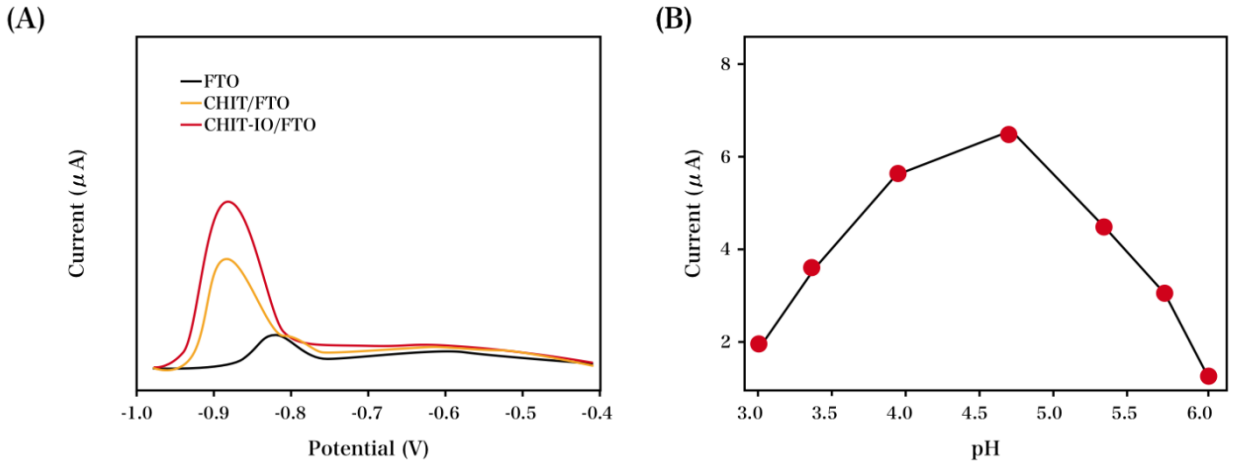

Figure 5. SWASVs of Cd(II) (20 μg/L) in an acetate buffer solution (0.1 M) with the CHIT-IO/FTO, CHIT/FTO and FTO electordes. (B) Effects of the pH of the supporting electrolyte.

Fig. 5B shows the effect of the pH (3.0–6.0) on the peak current of Cd(II). The current response increased as the pH value increased until a pH of 4.6. Further increasing the pH resulted in a decrease in the current. The interference of the hydrogen evolution with the deposition probably accounted for the responses recorded in the relatively acidic electrolyte. Moreover, there was a decrease in the number of ion-exchange sites because the effective deprotonation of the sulfonic groups in Nafion was not achieved under the exceedingly acidic conditions. Hence, the optimum pH value of 4.0 was fixed for further experiments.

The SWASV measurements were conducted under optimized conditions to study the sensitivity and the dynamic range of the proposed electrode. Fig. 6 shows a range of stripping responses after Cd(II) was consecutively added. The peak currents were shown to be linearly related to the Cd(II) concentration (1.0-100.0 μg/L). The LOD was 0.15 μg/L, which was calculated as three times the standard deviation of the blank signal ($S/N = 3$). The CHIT-IO/FTO electrode was compared with the

other electrodes for Cd(II) detection, as displayed in Table 1, and the proposed electrode showed a competitive linear range and a relatively lower LOD.

Table 1. Comparison of the electrodes for the detection of Cd(II).

Sensor	Method	Linear range (μg/L)	LOD (μg/L)	Reference
Sn film-modified CPE	SWASV	2-90	1.13	[40]
Bi powder-modified CPE	SWASV	10-100	1.2	[41]
Sn film-modified GCE	SWASV	10-110	1.1	[42]
CHIT-IO/FTO	SWASV	1-100	0.15	This work

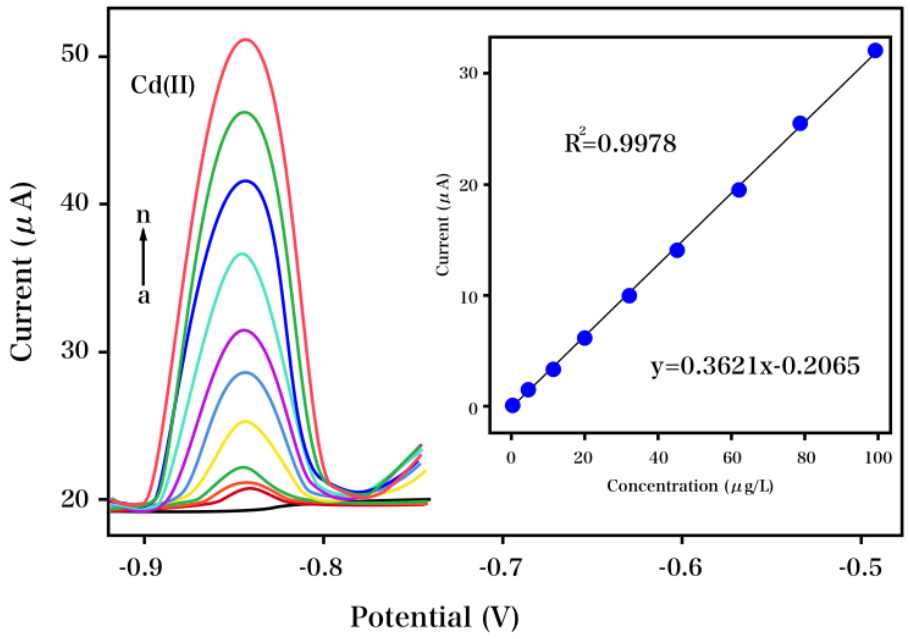

Figure 6. Voltammograms recorded after 0, 1, 5, 10, 20, 30, 40, 50, 60, 80, and 100 μg/L of Cd(II) was added at the CHIT-IO/FTO electrode, and the corresponding correlation is plotted in the inset.

The reproducibility of the developed electrode was evaluated by measuring a buffer solution. For a single electrode, the relative standard deviation (RSD) was 3.4% for five repetitive measurements. For the six different electrodes prepared using the same method, the RSD was 3.3%. When the radiation absorbed by a chemical element of interest is measured, the measurement of the amount of the chemical element in environmental specimens can be determined. This is known as inductively coupled plasma mass spectrometry (ICP-MS) which is a type of mass spectrometry which is capable of detecting metals and several non-metals at concentrations as low as one part in 10^{15} on non-interfered low-background isotopes. This is achieved by ionizing the sample with inductively coupled plasma and then using a mass spectrometer to separate and quantify those ions. The as-prepared CHIT-IO/FTO electrode was used to determine cadmium in soil specimens to assess whether the proposed electrode was feasible for an ordinary analysis. The standard addition technique was

employed to carry out the measurements, and the results were confirmed using ICP-MS assays and recovery experiments. As indicated in Table 2, these two techniques were consistent with each other with desirable recovery results, and the proposed technique was validated.

Table 2. Recovery experiments and comparison of the CHIT-IO/FTO electrode and ICP-MS for Cd(II) detection in several soil specimen extracts.

Sample	Soil concentration (mg/kg)	Added (mg/kg)	Found (mg/kg)	Found by ICP-MS(mg/kg)	Recovery (%)
Soil 1	0.65	0.5	1.147	1.148	99.74
		1.0	1.658	1.660	100.48
		2.0	2.644	2.645	99.76
Soil 2	0.58	0.5	1.574	1.577	99.77
		1.0	1.576	1.578	99.75
		2.0	2.581	2.577	99.40
Soil 3	0.72	0.5	1.222	1.218	100.04
		1.0	1.723	1.725	100.17
		2.0	2.714	2.720	99.78

7 different soil sample with different fertilizing amount were collected from orchard. The determination of the total Cd ions could be deduced from the diluted extract solution of soil. As shown in Table 3, the t test has been used for CHIT-IO/FTO electrode and ICP-MS comparison. After calculation, the average number d=0.1384, standard deviation is about 0.4574, standard error of mean difference s^d=0.1145, t=1.2151, where t is the degree of freedom df=15, $t_{0.05}$=2.12, $t_{0.01=2.94}$. Therefore, the determination of Cd ions in soil using both CHIT-IO/FTO electrode and ICP-MS has no significant difference.

Table 3. Total Cd ions content in soil determined by CHIT-IO/FTO electrode and ICP-MS methods (g/kg) n=2.

Method	Soil samples						
	1	2	3	4	5	6	7
ICP-MS	0.422	0781	0.293	1.500	1.086	0.955	1.478
CHIT-IO/FTO	0.406	0.766	0.285	1.485	1.147	0.974	1.522

4. CONCLUSIONS

This work successfully performed electrochemical sensing via the deposition of chitosan-iron oxide NPs onto FTO sheets. The CHIT-IO/FTO electrode was constructed to detect cadmium by means of SWASV. Herein, Cd(II) was sensitively detected by a dramatically sensitive electrode.

Furthermore, since the as-prepared electrode was remarkably conductive, it had a desirably enhanced electrochemical behaviour. Some corresponding parameters with respect to the operation and construction were optimized. The as-prepared electrode was also used for cadmium detection at trace levels in soil specimens and provided desirable results. As compared with the conventional ICP method, the proposed electrochemical approach showed a much quicker and simple advantages. Therefore, the proposed electrochemical sensor can be used for soil pollution determination. The traditional ICP-MS method requires 3-6 hours for soil sample preparation. The proposed CHIT-IO/FTO electrochemical sensor had a much quicker determination performance. The propose method could highly enhance the work efficacy. Moreover, this electrochemical approach did not require an expensive instrument. However, the proposed electrochemical sensor will be affected by the interference species. We will pit the effort to solve this problem in our next work.

ACKNOWLEDGEMENT
This work was supported by the special scientific research fund of agricultural public welfare profession of China (Grant No: 201203045-5): Key technology integration & demonstration of pollutants comprehensive control in farmland of bulk agricultural products.

References

1. G. Bertin and D. Averbeck, *Biochimie*, 88 (2006) 1549.
2. A. Afkhami, T. Madrakian, R. Ahmadi, H. Bagheri and M. Tabatabaee, *Microchim. Acta.*, 175 (2011) 69.
3. S. Cheng, *Environmental Science and Pollution Research*, 10 (2003) 192.
4. W.Q.Y. Dong, Y. Cui and X. Liu, *Soil and Sediment Contamination*, 10 (2001) 497.
5. B. Fang and X. Zhu, *Food control*, 39 (2014) 62.
6. Q. Wang, J. Liu and S. Cheng, *Environmental Monitoring and Assessment*, 187 (2015) 4178.
7. H. Bagheri, A. Afkhami, M. Saber-Tehrani and H. Khoshsafar, *Talanta*, 97 (2012) 87.
8. V.K. Gupta, M. Al Khayat, A.K. Singh and M.K. Pal, *Anal. Chim. Acta.*, 634 (2009) 36.
9. H. Bagheri, A. Afkhami, H. Khoshsafar, M. Rezaei and A. Shirzadmehr, *Sensors and Actuators B: Chemical*, 186 (2013) 451.
10. V. Gupta, A. Jain and P. Kumar, *Sensors and Actuators B: Chemical*, 120 (2006) 259.
11. V. Gupta, A. Singh, M. Al Khayat and B. Gupta, *Anal. Chim. Acta.*, 590 (2007) 81.
12. A. Afkhami, H. Bagheri, H. Khoshsafar, M. Saber-Tehrani, M. Tabatabaee and A. Shirzadmehr, *Anal. Chim. Acta.*, 746 (2012) 98.
13. B.C. Janegitz, L.C.S. Figueiredo-Filho, L.H. Marcolino-Junior, S.P. Souza, E.R. Pereira-Filho and O. Fatibello-Filho, *Journal of Electroanalytical Chemistry*, 660 (2011) 209.
14. V.K. Gupta, R. Jain, K. Radhapyari, N. Jadon and S. Agarwal, *Analytical Biochemistry*, 408 (2011) 179.
15. M. Hasanzadeh, A. Bahrami, M. Alizadeh and N. Shadjou, *RSC Advances*, 3 (2013) 24237.
16. N.J. Ronkainen and S.L. Okon, *Materials*, 7 (2014) 4669.
17. F. Xiao, L. Wang and H. Duan, *Biotechnology advances*, 34 (2016) 234.
18. M. Khadem, F. Faridbod, P. Norouzi, A.R. Foroushani, M.R. Ganjali and S.J. Shahtaheri, *JICS*, 13 (2016) 2077.
19. M. Govindhan, Z. Liu and A. Chen, *Nanomaterials*, 6 (2016) 211.
20. L.R. Schoukroun-Barnes, F.C. Macazo, B. Gutierrez, J. Lottermoser, J. Liu and R.J. White, *Annual Review of Analytical Chemistry*, 9 (2016) 163.
21. E. Dumitrescu and S. Andreescu, *Methods in Enzymology*, 589 (2017) 301.
22. M. Bäcker, C. Koch, S. Eiben, F. Geiger, F. Eber, H. Gliemann, A. Poghossian, C. Wege and M.J.

Schöning, *Sensors and Actuators B: Chemical*, 238 (2017) 716.
23. F. Tan, L. Cong, N.M. Saucedo, J. Gao, X. Li and A. Mulchandani, *J. Hazard. Mater.*, 320 (2016) 226.
24. A. Kaushik, P.R. Solanki, A.A. Ansari, B.D. Malhotra and S. Ahmad, *Biochemical Engineering Journal*, 46 (2009) 132.
25. N. Prabhakar, P.R. Solanki, A. Kaushik, M. Pandey and B. Malhotra, *Electroanalysis*, 22 (2010) 2672.
26. S. Singh, S.K. Arya, P. Pandey, B. Malhotra, S. Saha, K. Sreenivas and V. Gupta, *Applied Physics Letters*, 91 (2007) 063901.
27. A.A. Ansari, A. Kaushik, P. Solanki and B. Malhotra, *Electrochemistry Communications*, 10 (2008) 1246.
28. J. Graf, D. Taylor and J. Martinez, *Microscopy and Microanalysis*, 20 (2014) 1896.
29. Z. Yao, X. Yang, F. Wu, W. Wu and F. Wu, *Microchim. Acta.*, 183 (2016) 2799.
30. J.-K.F. Suh and H.W. Matthew, *Biomaterials*, 21 (2000) 2589.
31. A. Wang, C. Wang, L. Fu, W. Wong-Ng and Y. Lan, *Nano-Micro Letters*, 9 (2017) 47.
32. Y. Zheng, Z. Wang, F. Peng and L. Fu, *Inorganic and Nano-Metal Chemistry*, 47 (2017) 934.
33. Y. Zheng, Z. Wang, F. Peng and L. Fu, *Revista Mexicana de Ingeniería Química*, 16 (2017)
34. P.T.K. Loan, D. Wu, C. Ye, X. Li, V.T. Tra, Q. Wei, L. Fu, A. Yu, L.-J. Li and C.-T. Lin, *Biosensors and Bioelectronics*, 99 (2018) 85.
35. N. Kaur, H. Thakur, R. Kumar and N. Prabhakar, *Microchim. Acta.*, 183 (2016) 2307.
36. N. Kaur, H. Thakur and N. Prabhakar, *Journal of Electroanalytical Chemistry*, 775 (2016) 121.
37. P. Mallick and B.N. Dash, *Nanoscience and Nanotechnology*, 3 (2013) 130.
38. W. Hong, Q. He, S. Fan, M. Carl, H. Shao, J. Chen, E.Y. Chang and J. Du, *Magnetic Resonance in Medicine*, 78 (2017) 226.
39. H. Xu, L. Zeng, D. Huang, Y. Xian and L. Jin, *Food Chemistry*, 109 (2008) 834.
40. B.L. Li, Z.L. Wu, C.H. Xiong, H.Q. Luo and N.B. Li, *Talanta*, 88 (2012) 707.
41. S.B. Hočevar, I. Švancara, K. Vytřas and B. Ogorevc, *Electrochimica Acta*, 51 (2005) 706.
42. E. Tesarova, L. Baldrianova, S.B. Hocevar, I. Svancara, K. Vytras and B. Ogorevc, *Electrochimica Acta*, 54 (2009) 1506